Stem Cell Research 15 (2015) 655–664

Contents lists available at ScienceDirect

Stem Cell Research

journal homepage: www.elsevier.com/locate/scr

System-wide survey of proteomic responses of human bone marrow stromal cells (hBMSCs) to *in vitro* cultivation

Samuel T. Mindaye [a], Jessica Lo Surdo [b], Steven R. Bauer [b], Michail A. Alterman [a,*]

[a] Tumor Vaccines and Biotechnology Branch, Division of Cellular and Gene Therapies, Center for Biologics Evaluation and Research, US Food and Drug Administration, Silver Spring, MD, United States

[b] Cellular and Tissue Therapies Branch, Division of Cellular and Gene Therapies, Center for Biologics Evaluation and Research, US Food and Drug Administration, Silver Spring, MD, United States

ARTICLE INFO

Article history:
Received 27 April 2015
Received in revised form 21 September 2015
Accepted 26 September 2015
Available online 1 December 2015

ABSTRACT

Human bone marrow stromal cells (hBMSCs, also loosely called bone marrow-derived mesenchymal stem cells) are the subject of increasing numbers of clinical trials and laboratory research. Our group recently reported on the optimization of a workflow for a sensitive proteomic study of hBMSCs. Here, we couple this workflow with a label-free protein quantitation method to investigate the molecular responses of hBMSCs to long-term *in vitro* passaging. We explored the proteomic responses of hBMSCs by assessing the expression levels of proteins at early passage (passage 3, P3) and late passage (P7). We used multiple biological as well as technical replicates to ensure that the detected proteomic changes are repeatable between cultures and thus likely to be biologically relevant. Over 1700 proteins were quantified at three passages and a list of differentially expressed proteins was compiled. Bioinformatics-based network analysis and term enrichment revealed that metabolic pathways are largely altered, where many proteins in the glycolytic, pentose phosphate, and TCA pathways were shown to be largely upregulated in late passages. We also observed significant proteomic alterations in functional categories including apoptosis, and ER-based protein processing and sorting following *in vitro* cell aging. We posit that the comprehensive map outlined in this report of affected phenotypes as well as the underpinning molecular factors tremendously benefit the effort to uncovering targets that are not just used only to monitor cell fitness but can be employed to slowdown the *in vitro* aging process in hBMSCs and hence ensure manufacturing of cells with known quality, efficacy and stability.

Published by Elsevier B.V.

1. Background

Much of the recent attention paid to human bone marrow stromal cells (hBMSCs) is a consequence of their promise in cell-based therapy (Yi and Song, 2012). Features of BMSCs claimed that beneficial may include the capacity to home to sites of damage, differentiate into mature cells of the mesenchymal lineages, and secrete or stimulate the production of bioactive molecules. However, numerous studies have shown that extensive engraftment of BMSCs occurs rarely and thus they may act primarily through the release of soluble factors or through cell–cell interactions (Bernardo et al., 2012; Devine et al., 2003). Following their initial discovery in bone marrow, cells with similar surface characteristics have been isolated from many postnatal tissues (Otto and Wright, 2011), and these cells share common properties such as the capacity to adhere to plastic in cell culture and expression of common marker proteins (e.g., CD73, CD90, and CD105) or lack of other markers (e.g., CD11b, CD14, CD19, CD45, and HLA-DR) (Dominici et al., 2006; Keating, 2012). In bone marrow, they are a rare population (at times, from adult bone marrow only as few as 2000 BMSCs could be recovered) (Ksiazek, 2009). And yet, considerably higher cell numbers are often required for effective laboratory research or for clinical applications (10^6–10^9 cells per kg body weight (Wang et al., 2011; Yi and Song, 2012)). Hence, to obtain BMSCs in sufficient quantity, extensive *in vitro* culturing of primary cells is often necessary.

In regard to long-term culturing, the optimization of protocols continues to be a work in progress. One key challenge is the decline in cell fitness with *in vitro* passaging and this may impact the therapeutic benefit of BMSCs. For example, while early passage BMSCs support the expansion and differentiation of hematopoietic cells, the late passages (passage nine and beyond) did not exhibit this property (Briquet et al., 2010). Studies show that late passage BMSCs exhibit various indices of aging including altered growth kinetics with subsequent proliferation arrest, altered morphology and clonogenicity, diminished differentiation capacity, increased levels of reactive oxygen species (ROS), p21 and p53 (Bruder et al., 1997; Lo Surdo and Bauer, 2012; Lo Surdo et al., 2013; Wagner et al., 2008). These changes could be the result of reorganization at genomic, epigenetic, transcriptomic, and proteomic

* Corresponding author at: Tumor Vaccines and Biotechnology Branch, Division of Cellular and Gene Therapies, Center for Biologics Evaluation and Research, US FDA, Silver Spring, MD, United States.
E-mail address: Michail.Alterman@fda.hhs.gov (M.A. Alterman).

http://dx.doi.org/10.1016/j.scr.2015.09.013
1873-5061/Published by Elsevier B.V.

levels. BMSCs acquire chromosomal aberrations, albeit at a lower frequency, during passaging (4% in human BMSCs vs 9% in human pluripotent stem cells (hPSCs)) (Ben-David et al., 2011). Some transcriptome profiling experiments revealed that genes associated with cell death and chromatin assembly were up-regulated while those related to cell cycle, DNA repair, and DNA metabolism were largely down-regulated with *in vitro* aging (Bin Noh et al., 2010; Wagner et al., 2008). Meanwhile, epigenetic studies suggest that DNA-methylation changes better correlate with the *in vitro* cell aging than other genetic changes (Redaelli et al., 2012; Schellenberg et al., 2011).

Traditional 2D-gel based approaches have been applied to study various aspects of the BMSC proteome including differentiation-associated changes (Kasper et al., 2009; Sun et al., 2006), alterations in BMSCs as a result of disease (Seshi, 2006), changes initiated by mechanical stress (Yi et al., 2010), and the changes associated with *in vitro* cell passaging of BMSCs (Celebi and Elcin, 2009; Madeira et al., 2012). Taken together with other related studies, proteomic analyses undoubtedly provide important insights into the proteomic composition of BMSCs and help evolve our understanding about their biology. Nonetheless, more studies are needed, especially when many questions regarding the determinants of cell growth and development in culture media remain unanswered. In addition, molecular markers that correlate with developmental stages of cells, which may be utilized to monitor quality attributes of BMSCs, are yet to be revealed. Contemporary proteomic techniques are better placed to satisfy higher demands of characterizing complex biological systems than what could be achieved a few years ago. Such techniques combine the use of multidimensional chromatographic separation, high resolution mass spectrometry (MS), and improved bioinformatic data handling systems. The present work utilizes a workflow, which we recently optimized to survey the proteomics of human BMSCs and investigate the impact of long-term *in vitro* cultivation on protein expression in BMSCs. Based on multiple replicates; we performed an in-depth proteomic survey on hBMSCs at three passage stages (P3, P5 and P7). We used a label-free protein quantification technique to determine protein abundance and changes in response to long-term passaging. The technique uses the average intensity of the three most intense tryptic peptides per mole of a protein as surrogate to estimate protein abundance, a trend described by Silva et al. (2006). Our results provide detailed molecular insights of those changes that follow long-term *in vitro* cell passaging and offer potentially valuable protein targets for further studies to identify molecular markers that may correlate with hBMSC function.

2. Material and methods

2.1. Cell culture preparation

BMSCs from five human donors were purchased from commercially available sources (described in Ref. Mindaye et al., submitted for publication). According to the manufacturers, informed consent was received from donors and all participants fulfilled institutional requirements. Bone marrow aspirates were harvested and plastic adherent BMSCs were expanded. The time in culture prior to harvest was 15, 15, and 14 days for cultures 167696 (at 90% confluence), 110877 (at 45% confluence), and 8F3560 (at 35% confluence), respectively. At this stage, BMSCs were designated as passage zero (P0) by the supplier. These three cultures were further cultured to P1 for 6, 6, and 7 days, respectively, collected at 95% confluence, and frozen. P0 cells from PCBM1632 and PCBM1662 were in culture up to 80% confluence for 15 and 20 days, respectively before collection at P1. Results of the extensive characterization and authentication of all BMSCs were reported in previous publications (Lo Surdo and Bauer, 2012; Lo Surdo et al., 2013; Mindaye et al., 2013a, 2013b). Cells conform to specifications of the International Society for Cellular Therapy with regard to the expression of surface markers; namely, the expression of positive markers (≥90% positive for CD29, CD44, CD105, and CD166) and are negative for hematopoietic stem cell markers (Dominici et al., 2006). We also showed that these cells were capable of *in vitro* adipogenesis (Lo Surdo and Bauer, 2012; Lo Surdo et al., 2013).

P1 cells were plated at 60 cells/cm^2 in T175 flasks (Cellstar), culture-expanded in α-MEM (Invitrogen) supplemented with 16.5% fetal bovine serum (FBS) (JM Bioscience, San Diego, CA), L-glutamine and penicillin–streptomycin (Pen/strep) (Invitrogen), and cultured at 37 °C and 5% CO_2 as described earlier (Lo Surdo and Bauer, 2012; Lo Surdo et al., 2013). At 80% confluence, cells were harvested using 0.25% Trypsin/EDTA (Invitrogen), washed using phosphate buffered saline three times, snap frozen in liquid nitrogen, and stored at −80 °C at 5×10^6 cells at passages 3 (P3), 5 (P5), and 7 (P7) for later use. A passage number is the number of times cells were trypsinized prior to freezing. Respectively, the time to P3, P5, and P7 was: 167696 (8, 10, and 12 days), PCBM1632 (7, 9, and 17 days), 110877 (8, 9, and 10 days), 8F3560 (9, 10, 9 days), and PCBM1662 (10, 9, and 12 days). The same serum lot was used to expand all cell cultures for all passages. The cultures vary in their proliferation capacity, which generally decreases with passaging. The full proliferation characterization was described in previous publications (Lo Surdo and Bauer, 2012; Lo Surdo et al., 2013; Mindaye et al., 2013a).

2.2. Proteome preparation, nanoLC-MS^E analysis, data processing, and database searching

The detailed protocol for sample preparation, nanoLC-MS^E acquisition, Protein Lynx Global Surver (PLGS)-based data processing, database searching, and additional bioinformatic analyses are provided elsewhere (Mindaye et al., submitted for publication). Briefly, hBMSCs were lysed under SDS buffer conditions with the help of sonication and alternating pressure using a Barocycler (Pressure Biosciences, South Easton, MA). Cell lysates from culture 167696 and PCBM1632 were electrophoretically resolved into six fractions using the Gel-Eluted Liquid Fraction Entrapment Electrophoresis (GELFREE) system (Protein Discovery, Knoxville, TN) that allowed continuous separation of proteins through a gel-packed tube. Eluting proteins are trapped by a molecular weight cut-off membrane and subsequently collected in solution phase, which was suitable for downstream nanoLC-MS^E analysis. From 200 μg of total protein, six fractions were collected (procedure described in Ref. Mindaye et al., submitted for publication). Based on polyacrylamide gel electrophoresis, the first fraction was estimated to contain ~40% of the total protein loaded and each of the subsequent five fractions had ~12%. In the remaining three cell cultures the whole cell lysate was trypsinized without prior GELFREE fractionation. We excluded the upfront protein fractionation step for multiple reasons. First, the extra protein fractionation significantly increased the analysis time on the nanoLC-MS^E part. Secondly, a significantly higher protein amount is needed for the GELFREE fractionation step to produce sufficient material for downstream analyses. Furthermore, during protein fractionation, the migration of proteins through the gel is not necessarily sharp and proteins tend to tail between adjacent 1D gel fractions. The extent of such tailing varies between gel runs and thus might increase the error incurred during quantitative protein analysis. For samples processed without the protein fractionation step, we increased the number of fractions on the nanoLC part (described in Ref. Mindaye et al., submitted for publication).

The digest was eluted on a 2D nanoAcquity UPLC system with subsequent data-independent MS analysis (MS^E), which was carried out using SynaptG2 MS. MS^E data acquisition involves alternating the energy applied to the collision cell on a scan-by-scan basis without using an ion transmission window. This modality of data acquisition is expected to improve the overall depth of proteome coverage as it enables collection of data on precursor as well as product ion on all isotopes and charge states across the entire chromatographic peak width.

Data processing using PLGS correlates the precursor and product ion and the output was used to search against human SwissProt database. The detailed steps of time-alignment, ion accounting, correlation of precursor and product ion spectra, and database searching are described elsewhere (Geromanos et al., 2009; Li et al., 2009). A one-time randomized target database was used as decoy to calculate the false discovery rate of protein identification. Generally, the protein identification confidence was high as most proteins were identified using more than one peptide.

2.3. Label-free protein quantification, confirmation using flow cytometry, and bioinformatic analyses

The label-free protein quantification workflow relies on the average signal intensity of three most intense tryptic peptides per mole of a protein, an observation noted previously (Silva et al., 2006). Using this technique the relative concentration of proteins was determined and proteins whose expression levels at P5 and P7 were significantly different compared to the level at P3 (two-tailed t-test, p value ≤0.05) were identified. Further confirmation of differential expression was performed for some of the proteins using flow cytometry as an independent system. For this experiment, cells (cultures 167696 and PCBM1632) were thawed at either P3 or P7, cultured to 80% confluence, and incubated with 2.4G2 antibodies (ATCC) at 4 °C for 30 min to block non-specific binding. Then, fluorochrome-labeled antibodies (phycoerythrin [PE]; allophycocyanin [APC]; and fluorescein thiocyanate [FITC]) were added to aliquots of cells. Data were acquired using a FACS Canto II (BD Biosciences, San Jose, CA) flow cytometer and data analysis was completed using FlowJo Analysis Software (Tree Star, Ashland, OR).

Subcellular location prediction for identified proteins was performed using PANTHER server (Mi et al., 2013) and GProX was used for clustering analysis (Rigbolt et al., 2011). Biological function, protein network assignment, and other bioinformatic analyses were performed using either the Ingenuity Pathway Analysis application (IPA v9, Ingenuity Systems Inc., USA) or ArrayTrack data analysis and interpretation tool (www.fda.gov/ScienceResearch/BioinformaticsTools/Arraytrack). In IPA, Core Analyses were run using the focus protein sets (differentially expressed proteins) together with the corresponding fold changes using the default set parameters. Networks and biological functions were algorithmically generated and significance of each network and enriched functions was assessed using Fisher's exact test. Furthermore, the activation z-score, which is a measure of regulation of biological functions, was calculated based on experimentally observed functional changes that are compiled in the Ingenuity Knowledge Database (IKDB).

3. Results

3.1. The proteome of hBMSCs

In our previous reports, we established a robust workflow based on complementary MS techniques and developed a database that is larger than any database previously reported for hBMSC's proteome (Mindaye et al., 2013a, 2013b). There, we highlighted the proteomic basis of heterogeneity between cell cultures and identified proteins for which there was no prior evidence of expression on hBMSCs. The primary objective of the present study was to take advantage of the analytical platform we optimized and the database we constructed to further investigate the protein expression program in hBMSCs particularly during long-term *in vitro* culturing. Proteomic screening was performed at three passages (P3, P5, and P7). The dataset revealed at least 5000 proteins could be identified at each passage (see S1 and S1_Exp in Mindaye et al., submitted for publication). The dynamic range of proteins expressed in hBMSCs, as estimated using the average of protein-matched peptide intensity sum in triplicate runs at P3, spans 4 to 6 orders of magnitude (Fig. 1 in Mindaye et al., submitted for publication). This shows the expression-level variation of individual proteins in hBMSC. Structural proteins represent the major portion of the total proteomic signal, where proteins such as actins, vimentin, annexins, and histones alone accounted for over 50% of the total proteomic mass. Further, in order to assess the link between relative protein abundance and biological functions, we divided the proteome at P3 (PCBM1662) into five quantiles (Q1 through Q5) based on the estimated protein abundances. Bioinformatic gene ontology (GO) followed by Fisher's exact test extracted the search terms in each quantile, and terms with $p < 0.02$ are shown in Fig. 1. The most abundant proteins enrich biological functions in Q1 and the least abundant ones are represented by Q5. Proteins disulfide isomerase, reticulon, and thioredoxin have near median abundance values in Q1. Group Q2 can be exemplified by proteins such as ATP-dependent RNA helicase, HLA class I histocompatibility antigen, and ribosomal proteins, while in Q3 eukaryotic translation factor, basigin, and endophilin have near median estimated abundances. Papilin, chromobox protein homolog, and DNA replication licensing factor represent Q4, whereas transmembrane emp24 domain containing protein and peptidyl prolyl transisomerase are examples of proteins in Q5.

The enrichment shows the most abundant proteins in hBMSC are either glycolytic or involved in translation in ribosomes, transcription in spliceosomes, or have cellular communication functions through focal adhesion, tight, and adherence junctions. Core biological functions such as metabolism require proteins in a wider abundance range. Carbohydrate and protein metabolism is mostly executed by proteins in the moderate to higher abundance bracket, whereas metabolism of fatty acids and vitamins requires proteins in lower abundance. Functional categories involving protein folding, sorting, degradation, and transport are executed by proteins with high abundance as well as rare proteins. In addition, hBMSCs are thought to have an immunomodulatory role, and our analysis shows that proteins in the immune system network (e.g., leukocyte trans-endothelial migration, antigen processing and presentation) exist largely in higher abundance. It should be noted that these enrichment results are based on relative protein quantity estimation and primarily provides a general understanding as to how cell protein mass is allocated with regard to specific biological functions. Largely, our findings are consistent with results of similar studies that correlate protein abundance with biological functions in other human cells (Beck et al., 2011).

In total, over 5000 proteins per passage were identified (Mindaye et al., 2013a, and S1 in Mindaye et al., submitted for publication); of which 3218 were identified in all three passages and 1865 were identified only in either passage. From the 1865 proteins, 778 were identified only at P3, 725 at P5, and 362 at P7. Proteins with passage-dependent expression profiles were identified in fewer cell cultures and this owes to their lower abundance in hBMSC proteome. Only 275 proteins (35%) of the P3-associated proteins could be identified from three or more of the five cell sources. From the P5- and P7-specific proteins, 39% and 36% of them, respectively, followed similar passage-dependency in three or more occasions. Proteins mainly expressed in late passages include tumor protein p53 inducible protein 3 (TP53I3); an enzyme that is involved in cellular responses to oxidative stress. TP53P3 has been identified at P7 from samples 167696, PCBM1632, and PCBM1662 and could not be detected from the other cultures. The gene that encodes TP53I3 contains a p53 binding site and is activated by p53 and is involved in p53-mediated cell death and replicative senescence (Voltan et al., 2014). The transcription factor SOX18 (SRY-related HMG-box family) has also been identified only from passage P7 cells from all samples except from 110877 (Mindaye et al., 2013a, and S1 in Mindaye et al., submitted for publication). SOX18 is expressed in normal tissue as well as in cancer cells and it has been implicated in numerous biological processes including modulating stem cell proliferation, cell fate determination, cell maturation, and angiogenesis (Hoeth et al.,

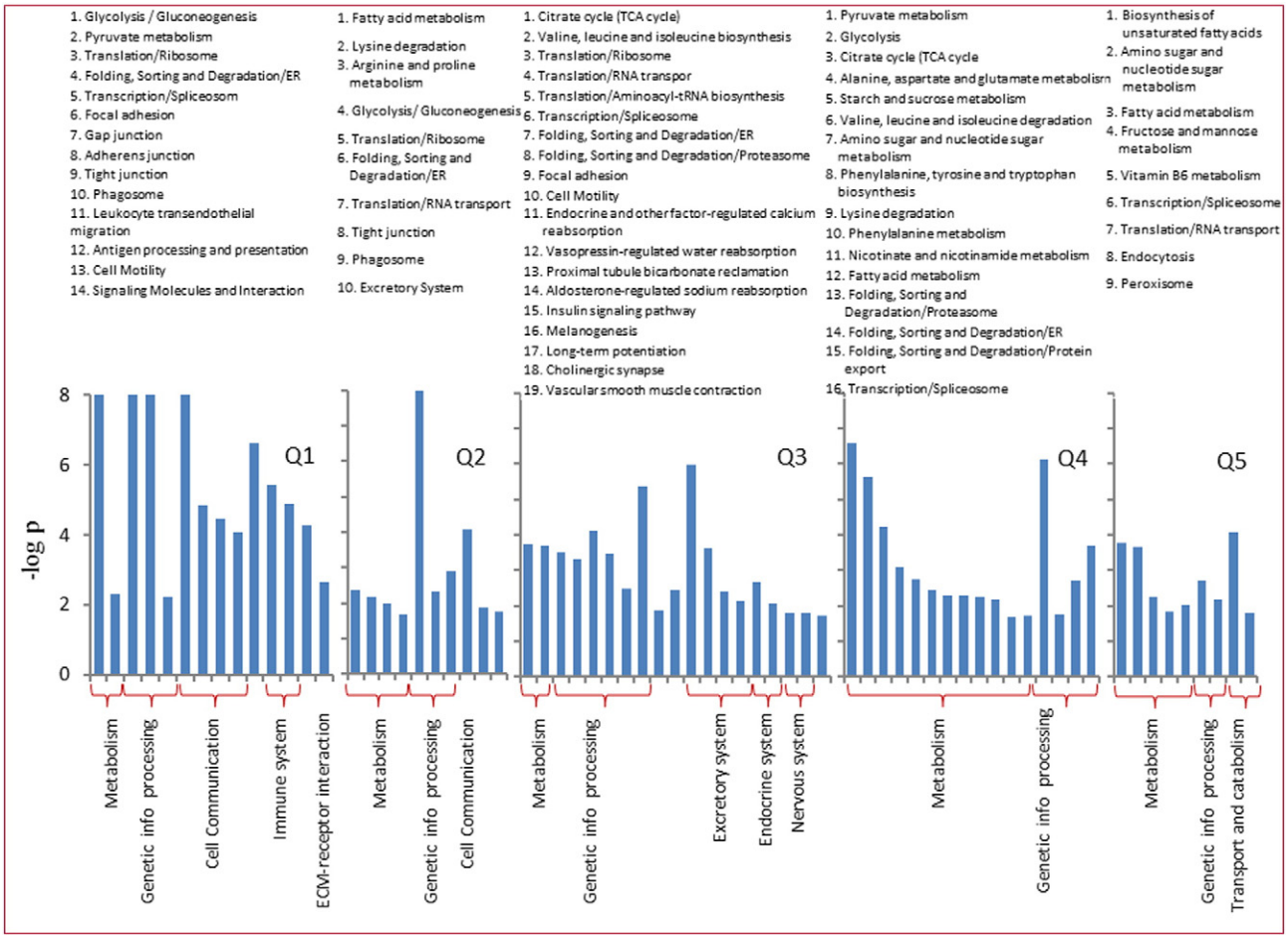

Fig. 1. GO enrichment based on protein abundance in hBMSCs (PCBM1662 at P3). The expression level of proteins was estimated using the average product ion intensity from triplicate runs and the proteome was divided into five equal quantiles (Q1 through Q5). Fisher's exact test extracted GO terms for each quantile and those with a p value ≤ 0.02 are listed on top of each quantile. These GO terms are represented by bars (from left to right) and the y-axes are the negative log of p values.

2012; Saitoh and Katoh, 2002). The set from late passages (P5 and P7) also include DDX20 (an RNA helicase that is associated with gene expression and induction of apoptosis), dual oxidase 1 (involved in oxidative stress), tousled-like kinase 2, and others with less understood biological functions.

3.2. Quantitative survey of protein expression profile in hBMSCs following expansion

The label-free protein quantitation method adopted in this study takes advantage of the linear relationship between MS signal response and protein concentration (Silva et al., 2006). The average signal count using three most intense tryptic peptides per mole of a protein corresponds to constant MS signal response. Therefore, using a known quantity of protein as an internal standard, the concentration of other detectable proteins in a digest can be estimated. In order to assess the suitability of this protein quantification method for such complex samples as hBMSC lysate, we spiked bovine catalase and alcohol dehydrogenase (ALDH) at the molar ratio of 2.75:1 to the hBMSC digest. Multiple runs of 2D nanoLC-MS^E were acquired. The MS signal response ratios of catalase and ALDH over multiple injections in separate days was determined to be stable with an overall 16% coefficient of variation (Fig. 2 in Ref. Mindaye et al., submitted for publication). Furthermore, as applied to the actual hBMSCs proteome, the run-to-run quantitative repeatability was fairly robust as demonstrated in Fig. 3 of Mindaye et al. (submitted for publication).

S1 and S1_Exp in Ref. Mindaye et al. (submitted for publication) summarize the identity and quantitative statistics of proteins identified from the five samples. For each culture, equal amount of total protein digest at P3, P5, and P7 was loaded onto a nanoLC column and the quantity of individual protein was calculated using catalase as the internal standard. For comparative purposes, the protein content at P3 was considered as the reference expression level, and thus a fold change is the ratio of on-column protein contents between P3 and later passages. In instances where low abundant proteins could be identified by less than three peptides, the fold changes were estimated using the normalized protein-matched peptide intensity sum. In this case, normalization was performed using the total precursor ion intensity of the internal standard (bovine catalase). There are also cases where proteins could be identified and quantified at one passage but could not be detected at others. Although failure to identify proteins at certain passages is most likely a matter of expression level difference rather than an on-or-off type of change, it is difficult to assign fold changes for such proteins. Thus, such proteins were not included in the differentially regulated proteins list during further bioinformatic enrichment.

Unsupervised clustering was carried out using the average fold changes of proteins at P5 and P7 (across five cultures). The GProX software partitioned the expression trend into six distinct clusters as shown in Fig. 3. The gene ontology search in KEGG database using ArrayTrack identified the corresponding biological functions that represent each cluster and the top most functions are listed at the bottom of each group. The clustering reveals most proteins appear to have reduced expression levels at P5 (Cluster 4 (112 proteins), C5 (161 proteins),

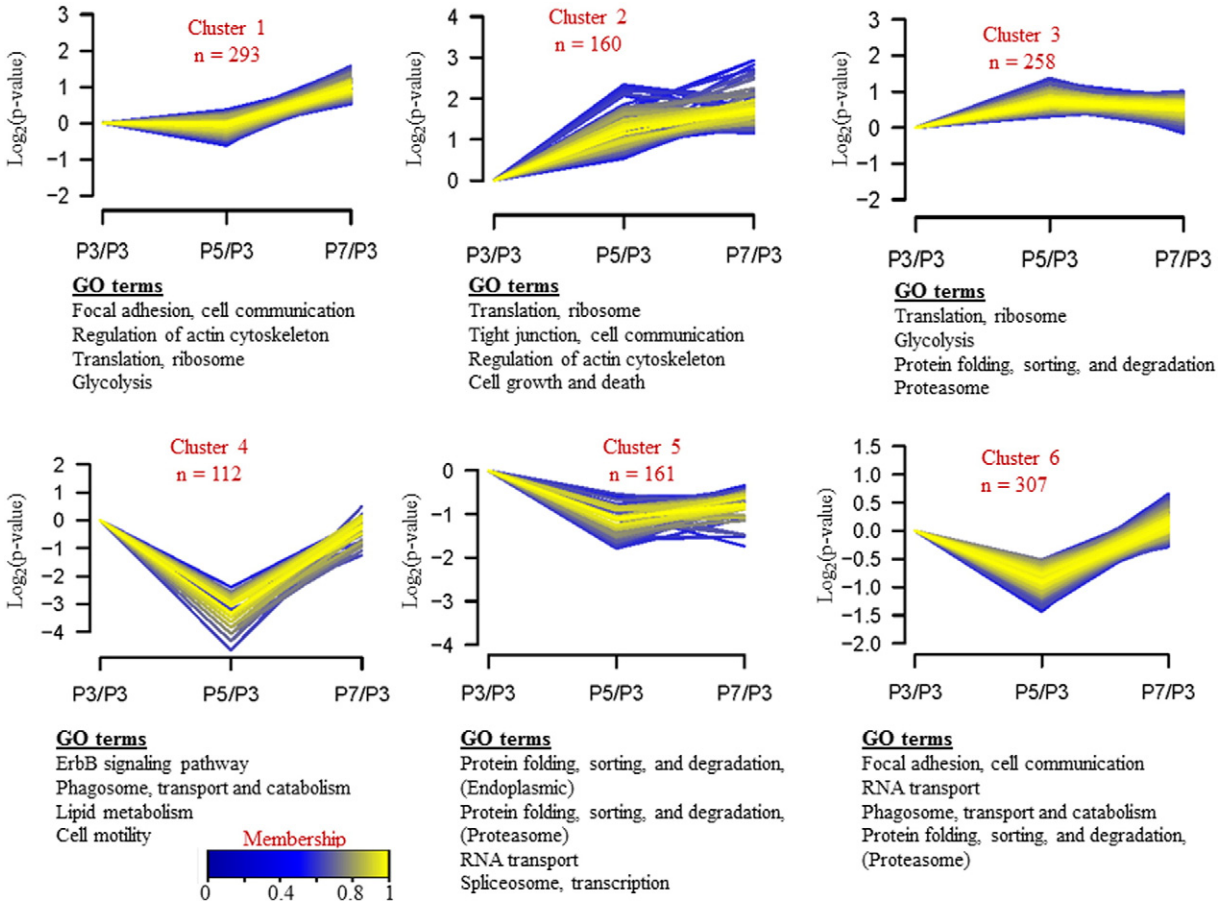

Fig. 2. Unsupervised clustering using GProX shows distinct protein expression patterns. The average fold changes on a $\log_2$ scale from five cultures (at P3, P5, and P7, where P3 is the reference level) were used for clustering. Upper and lower $\log_2$ limits of 0.58 and −0.32, which correspond to a 1.5 and −1.25 fold change, respectively, were considered the cut-off value. Membership value is the measure of how well a protein profile resembles the average cluster profile, where, a number close to one (yellow) indicates a profile closer to the average in the cluster.

and C6 (307 proteins)). The majority seem to return to the control level (expression at P3) when cells were further expanded to P7. Cluster 4 shows proteins whose content returned to the level similar to P3 and C6 has proteins expressed even at slightly higher level at P7 compared to P3. Cluster 5 represents the expression trend that remained lower at P7 as compared to P3. Similarly, clusters 1–3 represent proteins with an overall upward expression trend.

3.3. The expression of proteins in metabolic networks

One of the systematic changes identified by GO enrichment in KEGG database relates to the metabolic networks. Pathways including glycolysis, pentose phosphate pathway, pyruvate metabolism, and the citrate cycle all seem to be enriched with upregulated proteins (represented mostly by proteins in clusters 1 and 3). Proteins such as ENO2, ALDOC, PGK1, and LDHA (Table 1) are involved in the glycolytic pathway. Phosphofructokinase (PFK) catalyzes the conversion of fructose 6-phosphate and ATP to fructose 1,6-biphosphate and ADP. LDHA is another stable cytosolic enzyme that is very critical in the conversion of pyruvate to lactate. The concentration of LDHA in hBMSCs has nearly doubled at P7 as compared to P3. Higher concentration of LDHA reduces the accumulation of pyruvate and thus reduces the entry of pyruvate into oxidative metabolism. In effect, the up-regulation of LDHA reduces the accumulation of oxidative stress through the generation of mitochondrial ROS (Le et al., 2010). Further, pyruvate kinase (PK) is among the highly expressed proteins in hBMSCs and its expression increased by at least 1.5 fold at P7. PK catalyzes the final ATP-generation step in glycolysis. In tumor cells, the inactive PK maintains the flow of glycolytic intermediates into collateral pathways for synthesis of nucleic acids, amino acids, and lipids (Tamada et al., 2012). PK also plays roles during cell growth, proliferation and apoptosis; it senses nutritional scarcity (stress) during cell division and dissociates into an inactive form to protect cells from nutritional stress-dependent apoptosis (Gupta and Bamezai, 2010). Other enzymes such as aldolase C and phosphoglycerate mutase have also been observed to increase in expression level with passage number. From the pentose phosphate pathway, at least three proteins were upregulated at P7. Transldolase and aldolase C have shown more than two-fold increases as cells are cultured for extended periods. With regard to the TCA cycle and pyruvate metabolism, four proteins from each pathway experience an upward modulation pattern with *in vitro* culturing. Aldo-keto reductase nearly quadrupled and the concentration of citrate synthase increased by twofold.

3.4. Protein networks related to protein sorting, folding, and degradation

The protein networks in folding, sorting and degradation processes (proteasome and endoplasmic) are primarily represented by clusters C3, C5 and, C6. At P5 many endoplasmic reticulum (ER) proteins were down-regulated. Such proteins include dolichyl diphospho-oligosaccharide protein glycosyltransferase (OST48, average fold change −2.1), heat shock protein 90 alpha (HS90A, −2.6×), HS90B (−1.5×), HSP76 (−1.6×), protein disulfide isomerase A4 (PDIA4, −2.2×), and translocon-associated protein subunit delta

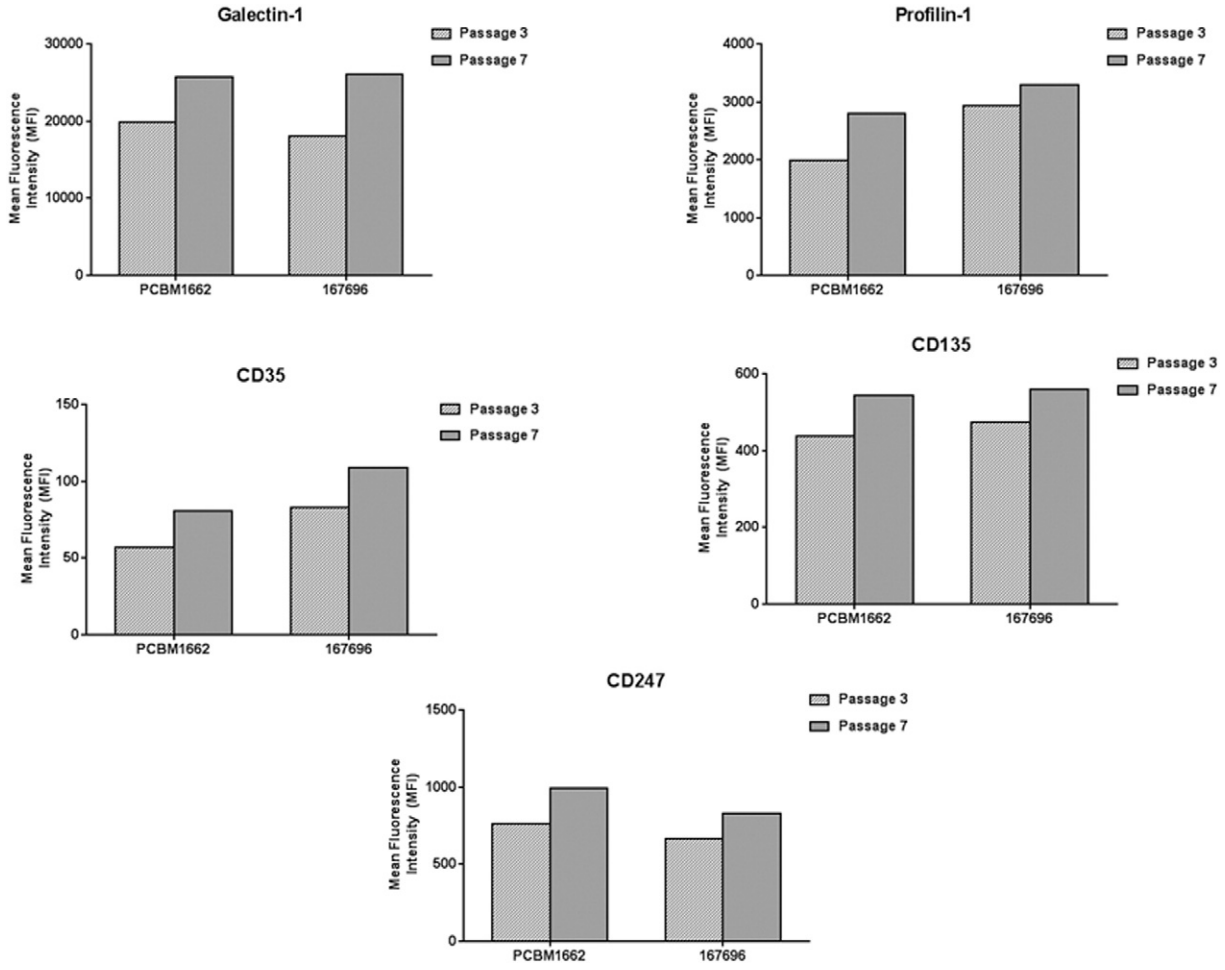

Fig. 3. Confirmation of differential expression of proteins by two hBMSC cultures using flow cytometry. The y-axes of the histograms show the mean fluorescent intensity and it is considered to be an estimate of the relative abundances of target proteins at P3 and P7. The differential expression profiles of galectin-1(4.4 fold) and profilin-1 (1.8 fold) with *in vitro* passaging were determined using LC-MS^E. Using MS, we also determined the expression of CD135, CD247, and several others for which there was no prior evidence for expression on hBMSCs (Mindaye et al., 2013a).

(SSR4, −1.3×) (S1 in Mindaye et al., submitted for publication). Proteins whose concentration at P5 increased include calreticulin (Calr, 1.5×), cytoskeletal associated protein 4 (CKAP4, 1.6×), heat shock related 70 kDa protein (HSPA2, 1.5×), ribosome binding protein 1 (RRBP1, 1.7×), and various proteasomes including subunit alpha type 1 (PSA1, 2.1×) (S1 in Mindaye et al., submitted for publication). At P7, most of these proteins remain modulated as in the case of Calr (2.6× compared to P3), HSP90AA1 (−1.7×), 60 kDa HSP (−1.7×), protein disulfide isomerase (PDI, −1.5×), and SSR4 (−1.4×). The ER lumen environment is considerably different from the cytosol and thus favors several protein modifications (e.g., glycosylation and disulfide bond formation). The ER protein processing system is controlled by a specialized set of chaperons including glucose regulated protein 78 (GRP78, BiP), GRP94, folding enzymes like protein disulfide isomerase, calnexin and calreticulin. The expression of BiP declines with age in various animal models (Rabek et al., 2003). In hBMSCs, BiP expression level decreased to close to 50% at P5 in three of the five cell cultures, while the reduction in the other two samples was not significant (S1 in Ref. Mindaye et al., submitted for publication). BiP is a member of the HSP70 family and its interaction with the hydrophobic domains of most proteins hinders misfolding during translocation to the ER (Naidoo, 2009). BiP is considered as the master regulator of ER stress response signaling (Naidoo, 2009). Further, PDI and Calr are responsible for the glycoprotein quality control system in cells (Naidoo, 2009). The binding of Calr to proteins in ER allows foldases and disulfide isomerase to catalyze the isomerization or exchange of disulfide bonds (Naidoo, 2009). The expression level of PDI at P7 was 1.5 fold lower than P3, while the content of Calr has increased by 2.5 fold (S1 in Ref. Mindaye et al., submitted for publication). An age-associated decline in PDI expression level has also been reported in numerous cases (Naidoo, 2009; Tomassini et al., 2004). Taken together, the alteration of key regulators of the ER and proteasome protein processing systems seems to suggest that there may be passage-associated disruption in the protein folding and surveillance system in hBMSCs. Not surprisingly, these protein processing systems are highly linked to multiple other signaling functions and thus their alteration may initiate other responses in cells. For example, the accumulation of aberrantly folded proteins can trigger apoptotic signaling events, alteration of cellular proliferation, or differentiation programs. It can also induce secondary effects by altering the cell-matrix interactions or affecting paracrine signaling (Tsang et al., 2010).

3.5. Proteins in the cell death and apoptotic signaling networks

Our analysis showed that proteins associated with the crucial functions of proliferation and cell death including necrosis and apoptosis were changed by extended cell culturing. When differentially regulated proteins between P3 and P7 were compared using IPA Core analysis, these cellular functions showed significant changes: proliferation of cells (p value 6.31E−8), cell death (3.58E−5), necrosis (4.42E−6), and apoptosis (1.28E−4). Table 7 of S1 in Ref. Mindaye et al. (submitted for publication) provides a summary of the differentially

Table 1
Differentially regulated proteins in the metabolic networks. A fold change is the ratio of on-column quantity of proteins at P5 and P7 with respect to P3. An average fold-change calculated using five cultures is shown.

ACCN	Symbol	Fold (P5/P3)	Fold (P7/P3)	Description
Glycolysis				
P09972	ALDOC	3.3	2.8	Aldolase C, fructose-bisphosphate
P09104	ENO2	0.9	1.9	Enolase 2 (gamma, neuronal)
P00338	LDHA	1.6	1.9	Lactate dehydrogenase A
P18669	PGAM1	1.5	2.1	Phosphoglycerate mutase 1
P00558	PGK1	1.3	1.5	Phosphoglycerate kinase 1
P14618	PKM2	1.4	1.5	Pyruvate kinase, muscle
Pentose phosphate pathway				
P37837	TALDO1	1.8	2.0	Transaldolase 1
O95336	PGLS	1.4	1.2	6-phosphogluconolactonase
P09972	ALDOC	3.3	2.8	Aldolase C, fructose-bisphosphate
Pyruvate metabolism				
P15121	AKR1B1	1.7	3.6	Aldo-keto reductase family 1
P40925	MDH1	1.5	2.4	Malate dehydrogenase 1, NAD
P00338	LDHA	1.6	1.9	Lactate dehydrogenase A
P14618	PKM2	1.4	1.5	Pyruvate kinase, muscle
Citrate cycle (TCA cycle)				
P53396	ACLY	1.3	1.3	ATP citrate lyase
Q99798	ACO2	1.2	2.1	Aconitase 2, mitochondrial
O75390	CS	1.7	2.0	Citrate synthase
P40925	MDH1	1.5	2.4	Malate dehydrogenase 1, NAD
Glyoxylate and dicarboxylate metabolism				
P40925	MDH1	1.5	2.4	Malate dehydrogenase 1, NAD
Q99798	ACO2	1.2	2.1	Aconitase 2, mitochondrial
O75390	CS	1.7	2.0	Citrate synthase

regulated proteins that are shown in prior experiments to influence apoptosis, proliferation and death events in cells (IKDB). The depletion of HSP27, HSP60, HSP70, and HSP90 has been shown to increase sensitivity to apoptotic stimuli (Lanneau et al., 2008). HSP90 regulates the activity and stability of apoptosis-implicated transcription factors including NF-kB, p53, Akt, Raf-1, and JNK (Lanneau et al., 2008). The depletion of only HSP70 in some cells stimulates a profound apoptotic response through caspase-3 activation (Lanneau et al., 2008). In hBMSCs, the expression of HSP70 and HSP90 was reduced by 50% or more in most cultures. GAPDH is another pro-apoptotic protein whose expression level almost quadrupled at P7. Besides metabolic function, GAPDH has roles in endocytosis, gene expression, tRNA transport, DNA repair, and replication (Yi et al., 2010). Among the cathepsins family, cathepsins B and D had higher expression levels at P7. These proteases have cell context-dependent influence on apoptotic signaling. Cathepsin D mediates the release of cytochrome C into the cytosol and activation of pro-caspase-3 and −9 (Liaudet-Coopman et al., 2006). In cancer cells, cathepsins have anti-apoptotic roles (Liaudet-Coopman et al., 2006).

Among the negative regulators of apoptosis, FHL-2 has the most fold change (3.1 fold increase). Studies have shown that FHL2 protects liver cells from doxorubicin-induced damage (Ng et al., 2011). Peroxiredoxin 6 (2.5 fold higher at P7) protects cells from apoptosis either through detoxifying ROS or interacting with caspase-8 and −10 (Choi et al., 2011). Gelsolin has both pro and anti-apoptotic roles depending on cell type and experimental conditions. In neutrophils, gelsolin is a substrate for caspase-3 and its cleavage facilitates the severing of actin filaments resulting in the dismantling of the membrane cytoskeleton, which is the hallmark of apoptosis. On the other hand, the intact gelsolin can interact with mitochondrial VDAC to inhibit the release of cytochrome C and subsequent apoptotic cascades (Leifeld et al., 2006). The expression of gelsolin and VDAC in hBMSCs increases by 2.5 and 2.3 fold, respectively. Furthermore, the level of superoxide dismutase (SOD) increases by almost 70% at P7 and this enzyme is known to block the activation of caspase cascade in response to apoptotic stimuli (Dimmeler et al., 1999).

3.6. Proteins in the growth and proliferation signaling networks

The proteomic networks related to cell growth and proliferation have also been altered significantly with passaging (see Table 7 of S1 in Ref. Mindaye et al., submitted for publication). For example, galectin 1 had higher expression level at P7. Galectin 1 interacts with α5β1 integrin, induces p21 transcription, and stabilizes p27, which results in G1 cell cycle arrest and growth inhibition (Camby et al., 2006). Galectin 1 role in hBMSC is to suppress the proliferation of T cells (Gieseke et al., 2010). Profilin is another ubiquitously expressed actin-binding protein whose expression in hBMSCs nearly doubles at P7. Reports show that profilin has an anti-proliferative effect partly by increasing the expression of CDK inhibitors (e.g., p27, kip 1) (Zou et al., 2010). Among the annexins, ANXA1, ANXA2, and ANXA5 have at least twice the protein levels by P7. While ANXA1 has a cell-type independent anti-proliferative action through sustained activation of ERK signaling cascade (Alldridge and Bryant, 2003), ANXA2 has a pro-proliferative role in human HeLa 293 cells (Chiang et al., 1999). Similarly, the level of four and a half LIM domain-containing proteins (FHL1 and FHL2) was significantly altered with passaging, where the content of FHL1 increased fourfold and FHL2 threefold. FHLs, through protein-protein interactions, influence apoptotic signaling and proliferation in a cell-dependent manner (Ding et al., 2009). In fibroblasts, FHL2 activates cyclin 1 and plays a positive role in cell proliferation; in tumor cells, the increased FHL2 expression inhibits proliferation by decreasing cyclin D1 content while increasing p21 expression (Labalette et al., 2008; Ng et al., 2011). In BMSCs, FHL2 control the osteogenic differentiation and bone formation through modulation of Wnt molecules (Brun et al., 2013).

3.7. Confirmation of expression changes using flow cytometry

To further confirm the expression changes detected using label-free MS^E technique, independent experiments using flow cytometry in conjunction with polyclonal antibodies were run for galectin 1 and profilin using samples 167696 and PCBM1662 at P3 and P7. The measurements determined the populations of cells that express target proteins and helped estimate the protein abundances at P7 in relation to P3 (Fig. 2). Furthermore, we previously reported the expression of at least 14 new CDs for which there was no prior evidence of expression on hBMSCs (Mindaye et al., 2013a). To provide more evidence of their expression and study their expression changes in relation to cell passaging, we also included three CDs (CD135, CD243, and CD247) in these flow cytometry experiments. Fig. 2 summarizes the relative expressions of target proteins at P3 in relation to P7. The mean fluorescence intensities were used to estimate the relative expression levels. Conformingly, the expression changes based on flow cytometry and label-free MS technique follows similar trends although the changes determined using flow measurements are slightly lower than those obtained using LC-MS^E approach. For example, galectin 1 increases by at least fourfold based on MS data but an average of 1.4 fold increase (1.3× for PCBM1662 and 1.4× for 167696) was determined using flow cytometry.

4. Discussion

Aging-associated phenotype change in hBMSCs is one of the most important considerations in furthering the advancement of cell-based therapy and is a subject of numerous studies and reviews (Baker et al., 2015; Bara et al., 2014). In regard to the *in vivo* aging, there is a general agreement between most studies in that the cell fitness declines with aging. For example, with age of the bone marrow the frequency of CFUs declines, susceptibility to senescence increase, and cells have reduced migration and adhesion capacity (Baker et al., 2015). The clinical performance of BMSCs from aged individuals has also been shown in most instances to be less than cells from younger counterparts (Baker et al., 2015). *In vitro* aging is also very critical in influencing therapy

because manufacturing of hBMSCs in a quantity suitable for clinical use requires extensive *in vitro* expansion of cells. *In vitro* culturing exposes cells to numerous artificial stresses. For example, harvesting cells using enzymatic treatment (usually trypsin, collagenase, accutase, or mixture of them) exposes cells to a condition where the surface proteins could be partially cleaved and this may initiate a cascade of biological events (Huang et al., 2010). The effect of *in vitro* passaging on hBMSC's phenotype has been examined in numerous occasions (Bruder et al., 1997; Lo Surdo and Bauer, 2012; Lo Surdo et al., 2013; Wagner et al., 2010). We also observed, among others, that metabolic pathways are largely altered, where many proteins in the glycolytic, pentose phosphate, and TCA pathways were shown to be largely upregulated in late passages. An expression trend similar to ours for some of the proteins has already been reported by other authors. Using 2D gel techniques, Sun and coworkers showed the expression levels of pyruvate kinase and enolase increase with serial sub-culturing of hBMSCs (Sun et al., 2006). In a separate report, Madeira et al. used a comparable technique to report similar induction of GAPDH, aldolase, and aldo-keto reductase with *in vitro* aging of cells (Madeira et al., 2012).

Proteins in the metabolic networks are traditionally considered to have housekeeping functions, although this notion has recently evolved as they are recognized to play vital roles in proliferation, self-renewal, differentiation, and aging (Shyh-Chang et al., 2013). For example, hiPSCs experience a high glycolytic flux during oxidative stress. During differentiation of hiPSCs, genes in the pentose phosphate and lipid biosynthesis pathways become upregulated (Zhang et al., 2012). Further, one of the changes during reprograming of somatic cells is the progressive increase in glycolytic genes. In fact, the metabolic network is claimed to be the major barrier during reprograming (Hansson et al., 2012; Zhang et al., 2012). The metabolic network has also been shown to play important roles in hBMSC biology. Glycolysis is the major source of energy during chondrogenic differentiation and hypoxia suppresses osteogenic differentiation of hBMSCs (Pattappa et al., 2011). In regards to self-renewal and expansion, some reports have already indicated that the underlying metabolic pathways have a significant effect on population doublings, frequency of primitive cells in a colony, colony size, and number of colonies in culture media (Estrada et al., 2012; Pattappa et al., 2011; Sanchez-Arago et al., 2013). BMSCs retain the flexibility to use both oxidative phosphorylation and glycolytic pathways (Pattappa et al., 2011; Schop et al., 2009). Under normoxic conditions, non-differentiating BMSCs depend more on glycolysis (~70%) and part of the reason may be that cells require not just ATP, but also other metabolic byproducts. Besides, glycolysis protects cells from excessive generation of ROS, the primary cause of cellular damage and senescence (Pattappa et al., 2011; Shyh-Chang et al., 2013). The fact that enzyme content in the glycolytic network increased with passage seems to indicate that glycolytic pathway may be preferred even more so as hBMSCs are subjected to stress caused by long-term passaging. Interestingly, gene expression assays in BMSCs also pointed to similar bioenergetic alteration trends with passaging (Will, 2010). Therefore, as we seek to gain clearer understanding of the relationship between metabolic networks and some key features of hBMSCs; the differentially regulated metabolic enzymes identified in this study may be key starting targets.

We also observed the alteration of proteomic networks related to the apoptotic and proliferative pathways. Senescence and apoptosis are essential mechanisms for cells to respond to the changing environment. Apoptosis involves intricate proteomic networks and Table 7 of S1 in Ref. Mindaye et al., (submitted for publication) summarizes modulated proteins in hBMSCs that are linked in prior studies with apoptosis (IKDB). Some of these are pro- and others are anti-apoptotic proteins. Stress-related heat shock proteins have been markedly reduced at P7, observations consistent with expectations (Madeira et al., 2012). GAPDH is another important pro-apoptotic protein whose expression level almost quadrupled at P7. During apoptosis, its expression and mitochondrial accumulation increases and this leads to increased membrane permeability with subsequent release of pro-apoptotic proteins (Tarze et al., 2007). Based on systematic IPA analysis, apoptosis has an overall activation z score of 1.6 (the fold change that this biological function increased at P7 as compared to P3). Other cellular events with similar biological tendencies are cell death and necrosis, each with activation z-scores of 2.1 and 1.8, respectively. Moreover, proteins involved in cell growth and proliferation have also experienced passage-dependent expression patterns (p value $6.31E-8$). The overall decline in proliferation capacity has −0.60 z-score, indicating P7 cells become somewhat less proliferative than P3. These results correlate with the significant reduction in the frequency of CFUs or increase in time to 80% confluence of all hBMSC samples with passaging except 8F3560, which had fairly constant CFUs across passaging (Lo Surdo et al., 2013). According to the IKDB, some of the proliferation-associated proteins are pro-proliferative (e.g., nucleolin); however, most are anti-proliferative (e.g., galectin 1 and annexin 1), and the effect on proliferation for some proteins is cell context-dependent (e.g., annexin 2).

Taken together, hBMSC-based therapy and research depend highly on the isolation and manufacturing of cells with predictable biological functions in large numbers. We extensively explored the underpinning molecular factors that influence the age-associated phenotype changes in hBMSCs. Using a robust label-free quantitative proteomic approach, the study mapped the expression changes associated with long-term passaging in five hBMSC cultures derived from different human donors. Over 1700 proteins were quantified at three passages and a differentially expressed protein list was identified. Bioinformatic-based network analysis and term enrichment helped to identify altered biological functions. We documented that culturing stimulates extensive proteomic alterations in functional categories including apoptosis, ER-based protein processing and sorting, and metabolic pathways. Identification of these affected biological functions together with the underlying molecular networks tremendously benefit the effort to uncovering targets that are not just used to monitor cell fitness but that can also be employed to slowdown the *in vitro* aging process in hBMSCs and hence ensure manufacturing of cells with known quality, efficacy and stability.

Author contributions

STM — acquisition, analysis and interpretation of data, drafting the article and final approval of the version to be published; JLS — acquisition of data, revising the article and final approval of the version to be published; SRB — conception and design of the study, revising the article and final approval of the version to be published; MAA — conception and design of the study, analysis and interpretation of data, drafting and revising the article and final approval of the version to be published.

Appendix A. Supplementary data

Supplementary data to this article can be found online at http://dx.doi.org/10.1016/j.scr.2015.09.013.

References

Alldridge, L.C., Bryant, C.E., 2003. Annexin 1 regulates cell proliferation by disruption of cell morphology and inhibition of cyclin D1 expression through sustained activation of the ERK1/2 MAPK signal. Exp. Cell Res. 290, 93–107.

Baker, N., Boyette, L.B., Tuan, R.S., 2015. Characterization of bone marrow-derived mesenchymal stem cells in aging. Bone 70, 37–47.

Bara, J.J., Richards, R.G., Alini, M., Stoddart, M.J., 2014. Concise review: bone marrow-derived mesenchymal stem cells change phenotype following in vitro culture: implications for basic research and the clinic. Stem Cells 32, 1713–1723.

Beck, M., Schmidt, A., Malmstroem, J., Claassen, M., Ori, A., Szymborska, A., Herzog, F., Rinner, O., Ellenberg, J., Aebersold, R., 2011. The quantitative proteome of a human cell line. Mol. Syst. Biol. 7, 549.

Ben-David, U., Mayshar, Y., Benvenisty, N., 2011. Large-scale analysis reveals acquisition of lineage-specific chromosomal aberrations in human adult stem cells. Cell Stem Cell 9, 97–102.

Bernardo, M.E., Pagliara, D., Locatelli, F., 2012. Mesenchymal stromal cell therapy: a revolution in regenerative medicine? Bone Marrow Transplant. 47, 164–171.
Bin Noh, H., Ahn, H.J., Lee, W.J., Kwack, K., Do Kwon, Y., 2010. The molecular signature of in vitro senescence in human mesenchymal stem cells. Genes Genomics 32, 87–93.
Briquet, A., Dubois, S., Bekaert, S., Dolhet, M., Beguin, Y., Gothot, A., 2010. Prolonged ex vivo culture of human bone marrow mesenchymal stem cells influences their supportive activity toward NOD/SCID-repopulating cells and committed progenitor cells of B lymphoid and myeloid lineages. Haematologica 95, 47–56.
Bruder, S.P., Jaiswal, N., Haynesworth, S.E., 1997. Growth kinetics, self-renewal, and the osteogenic potential of purified human mesenchymal stem cells during extensive subcultivation and following cryopreservation. J. Cell. Biochem. 64, 278–294.
Brun, J., Fromigue, O., Dieudonne, F.X., Marty, C., Chen, J., Dahan, J., Wei, Y., Marie, P.J., 2013. The LIM-only protein FHL2 controls mesenchymal cell osteogenic differentiation and bone formation through Wnt5a and Wnt10b. Bone 53, 6–12.
Camby, I., Le Mercier, M., Lefranc, F., Kiss, R., 2006. Galectin-1: a small protein with major functions. Glycobiology 16, 137R–157R.
Celebi, B., Elcin, Y.M., 2009. Proteome analysis of rat bone marrow mesenchymal stem cell subcultures. J. Proteome Res. 8, 2164–2172.
Chiang, Y., Rizzino, A., Sibenaller, Z.A., Wold, M.S., Vishwanatha, J.K., 1999. Specific down-regulation of annexin II expression in human cells interferes with cell proliferation. Mol. Cell. Biochem. 199, 139–147.
Choi, H., Chang, J.W., Jung, Y.K., 2011. Peroxiredoxin 6 interferes with TRAIL-induced death-inducing signaling complex formation by binding to death effector domain caspase. Cell Death Differ. 18, 405–414.
Devine, S.M., Cobbs, C., Jennings, M., Bartholomew, A., Hoffman, R., 2003. Mesenchymal stem cells distribute to a wide range of tissues following systemic infusion into nonhuman primates. Blood 101, 2999–3001.
Dimmeler, S., Hermann, C., Galle, J., Zeiher, A.M., 1999. Upregulation of superoxide dismutase and nitric oxide synthase mediates the apoptosis-suppressive effects of shear stress on endothelial cells. Arterioscler. Thromb. Vasc. Biol. 19, 656–664.
Ding, L., Wang, Z., Yan, J., Yang, X., Liu, A., Qiu, W., Zhu, J., Han, J., Zhang, H., Lin, J., et al., 2009. Human four-and-a-half LIM family members suppress tumor cell growth through a TGF-beta-like signaling pathway. J. Clin. Invest. 119, 349–361.
Dominici, M., Le Blanc, K., Mueller, I., Slaper-Cortenbach, I., Marini, F., Krause, D., Deans, R., Keating, A., Prockop, D., Horwitz, E., 2006. Minimal criteria for defining multipotent mesenchymal stromal cells. The International Society for Cellular Therapy position statement. Cytotherapy 8, 315–317.
Estrada, J.C., Albo, C., Benguria, A., Dopazo, A., Lopez-Romero, P., Carrera-Quintanar, L., Roche, E., Clemente, E.P., Enriquez, J.A., Bernad, A., et al., 2012. Culture of human mesenchymal stem cells at low oxygen tension improves growth and genetic stability by activating glycolysis. Cell Death Differ. 19, 743–755.
Geromanos, S.J., Vissers, J.P., Silva, J.C., Dorschel, C.A., Li, G.Z., Gorenstein, M.V., Bateman, R.H., Langridge, J.I., 2009. The detection, correlation, and comparison of peptide precursor and product ions from data independent LC–MS with data dependant LC–MS/MS. Proteomics 9, 1683–1695.
Gieseke, F., Bohringer, J., Bussolari, R., Dominici, M., Handgretinger, R., Muller, I., 2010. Human multipotent mesenchymal stromal cells use galectin-1 to inhibit immune effector cells. Blood 116, 3770–3779.
Gupta, V., Bamezai, R.N., 2010. Human pyruvate kinase M2: a multifunctional protein. Protein Sci. 19, 2031–2044.
Hansson, J., Rafiee, M.R., Reiland, S., Polo, J.M., Gehring, J., Okawa, S., Huber, W., Hochedlinger, K., Krijgsveld, J., 2012. Highly coordinated proteome dynamics during reprogramming of somatic cells to pluripotency. Cell Rep. 2, 1579–1592.
Hoeth, M., Niederleithner, H., Hofer-Warbinek, R., Bilban, M., Mayer, H., Resch, U., Lemberger, C., Wagner, O., Hofer, E., Petzelbauer, P., et al., 2012. The transcription factor SOX18 regulates the expression of matrix metalloproteinase 7 and guidance molecules in human endothelial cells. PLoS One 7, e30982.
Huang, H.L., Hsing, H.W., Lai, T.C., Chen, Y.W., Lee, T.R., Chan, H.T., Lyu, P.C., Wu, C.L., Lu, Y.C., Lin, S.T., et al., 2010. Trypsin-induced proteome alteration during cell subculture in mammalian cells. J. Biomed. Sci. 17, 36.
Kasper, G., Mao, L., Geissler, S., Draycheva, A., Trippens, J., Kuhnisch, J., Tschirschmann, M., Kaspar, K., Perka, C., Duda, G.N., et al., 2009. Insights into mesenchymal stem cell aging: involvement of antioxidant defense and actin cytoskeleton. Stem Cells 27, 1288–1297.
Keating, A., 2012. Mesenchymal stromal cells: new directions. Cell Stem Cell 10, 709–716.
Ksiazek, K., 2009. A comprehensive review on mesenchymal stem cell growth and senescence. Rejuvenation Res. 12, 105–116.
Labalette, C., Nouet, Y., Sobczak-Thepot, J., Armengol, C., Levillayer, F., Gendron, M.C., Renard, C.A., Regnault, B., Chen, J., Buendia, M.A., et al., 2008. The LIM-only protein FHL2 regulates cyclin D1 expression and cell proliferation. J. Biol. Chem. 283, 15201–15208.
Lanneau, D., Brunet, M., Frisan, E., Solary, E., Fontenay, M., Garrido, C., 2008. Heat shock proteins: essential proteins for apoptosis regulation. J. Cell. Mol. Med. 12, 743–761.
Le, A., Cooper, C.R., Gouw, A.M., Dinavahi, R., Maitra, A., Deck, L.M., Royer, R.E., Vander Jagt, D.L., Semenza, G.L., Dang, C.V., 2010. Inhibition of lactate dehydrogenase a induces oxidative stress and inhibits tumor progression. Proc. Natl. Acad. Sci. U. S. A. 107, 2037–2042.
Leifeld, L., Fink, K., Debska, G., Fielenbach, M., Schmitz, V., Sauerbruch, T., Spengler, U., 2006. Anti-apoptotic function of gelsolin in fas antibody-induced liver failure in vivo. Am. J. Pathol. 168, 778–785.
Li, G.Z., Vissers, J.P., Silva, J.C., Golick, D., Gorenstein, M.V., Geromanos, S.J., 2009. Database searching and accounting of multiplexed precursor and product ion spectra from the data independent analysis of simple and complex peptide mixtures. Proteomics 9, 1696–1719.
Liaudet-Coopman, E., Beaujouin, M., Derocq, D., Garcia, M., Glondu-Lassis, M., Laurent-Matha, V., Prebois, C., Rochefort, H., Vignon, F., 2006. Cathepsin D: newly discovered functions of a long-standing aspartic protease in cancer and apoptosis. Cancer Lett. 237, 167–179.
Lo Surdo, J., Bauer, S.R., 2012. Quantitative approaches to detect donor and passage differences in adipogenic potential and clonogenicity in human bone marrow-derived mesenchymal stem cells. Tissue Eng. Part C Methods 18, 877–889.
Lo Surdo, J.L., Millis, B.A., Bauer, S.R., 2013. Automated microscopy as a quantitative method to measure differences in adipogenic differentiation in preparations of human mesenchymal stromal cells. Cytotherapy 15, 1527–1540.
Madeira, A., da Silva, C.L., dos Santos, F., Camafeita, E., Cabral, J.M., Sa-Correia, I., 2012. Human mesenchymal stem cell expression program upon extended ex-vivo cultivation, as revealed by 2-DE-based quantitative proteomics. PLoS One 7, e43523.
Mi, H., Muruganujan, A., Casagrande, J.T., Thomas, P.D., 2013. Large-scale gene function analysis with the PANTHER classification system. Nat. Protoc. 8, 1551–1566.
Mindaye, S.T., Ra, M., Lo Surdo, J., Bauer, S.R., Alterman, M.A., 2015. The proteomic dataset for bone marrow derived mesenchymal stromal cells: the effect of in vitro passaging. Data in Brief (submitted for publication).
Mindaye, S.T., Ra, M., Lo Surdo, J., Bauer, S.R., Alterman, M.A., 2013a. Improved proteomic profiling of the cell surface of culture-expanded human bone marrow multipotent stromal cells. J. Proteome 78, 1–14.
Mindaye, S.T., Ra, M., Lo Surdo, J.L., Bauer, S.R., Alterman, M.A., 2013b. Global proteomic signature of undifferentiated human bone marrow stromal cells: evidence for donor-to-donor proteome heterogeneity. Stem Cell Res. 11, 793–805.
Naidoo, N., 2009. ER and aging-protein folding and the ER stress response. Ageing Res. Rev. 8, 150–159.
Ng, C.F., Ng, P.K., Lui, V.W., Li, J., Chan, J.Y., Fung, K.P., Ng, Y.K., Lai, P.B., Tsui, S.K., 2011. FHL2 exhibits anti-proliferative and anti-apoptotic activities in liver cancer cells. Cancer Lett. 304, 97–106.
Otto, W.R., Wright, N.A., 2011. Mesenchymal stem cells: from experiment to clinic. Fibrogenesis Tissue Repair 4, 20.
Pattappa, G., Heywood, H.K., de Bruijn, J.D., Lee, D.A., 2011. The metabolism of human mesenchymal stem cells during proliferation and differentiation. J. Cell. Physiol. 226, 2562–2570.
Rabek, J.P., Boylston III, W.H., Papaconstantinou, J., 2003. Carbonylation of ER chaperone proteins in aged mouse liver. Biochem. Biophys. Res. Commun. 305, 566–572.
Redaelli, S., Bentivegna, A., Foudah, D., Miloso, M., Redondo, J., Riva, G., Baronchelli, S., Dalpra, L., Tredici, G., 2012. From cytogenomic to epigenomic profiles: monitoring the biologic behavior of in vitro cultured human bone marrow mesenchymal stem cells. Stem Cell Res. Ther. 3, 47.
Rigbolt, K.T., Vanselow, J.T., Blagoev, B., 2011. GProX, a user-friendly platform for bioinformatics analysis and visualization of quantitative proteomics data. Mol. Cell. Proteomics 10 (O110), 007450.
Saitoh, T., Katoh, M., 2002. Expression of human SOX18 in normal tissues and tumors. Int. J. Mol. Med. 10, 339–344.
Sanchez-Arago, M., Garcia-Bermudez, J., Martinez-Reyes, I., Santacatterina, F., Cuezva, J.M., 2013. Degradation of IF1 controls energy metabolism during osteogenic differentiation of stem cells. EMBO Rep. 14, 638–644.
Schellenberg, A., Lin, Q., Schuler, H., Koch, C.M., Joussen, S., Denecke, B., Walenda, G., Pallua, N., Suschek, C.V., Zenke, M., et al., 2011. Replicative senescence of mesenchymal stem cells causes DNA-methylation changes which correlate with repressive histone marks. Aging (Albany NY) 3, 873–888.
Schop, D., Janssen, F.W., van Rijn, L.D., Fernandes, H., Bloem, R.M., de Bruijn, J.D., van Dijkhuizen-Radersma, R., 2009. Growth, metabolism, and growth inhibitors of mesenchymal stem cells. Tissue Eng. A 15, 1877–1886.
Seshi, B., 2006. An integrated approach to mapping the proteome of the human bone marrow stromal cell. Proteomics 6, 5169–5182.
Shyh-Chang, N., Daley, G.Q., Cantley, L.C., 2013. Stem cell metabolism in tissue development and aging. Development 140, 2535–2547.
Silva, J.C., Gorenstein, M.V., Li, G.Z., Vissers, J.P., Geromanos, S.J., 2006. Absolute quantification of proteins by LCMSE: a virtue of parallel MS acquisition. Mol. Cell. Proteomics 5, 144–156.
Sun, H.J., Bahk, Y.Y., Choi, Y.R., Shim, J.H., Han, S.H., Lee, J.W., 2006. A proteomic analysis during serial subculture and osteogenic differentiation of human mesenchymal stem cell. J. Orthop. Res. 24, 2059–2071.
Tamada, M., Suematsu, M., Saya, H., 2012. Pyruvate kinase M2: multiple faces for conferring benefits on cancer cells. Clin. Cancer Res. 18, 5554–5561.
Tarze, A., Deniaud, A., Le Bras, M., Maillier, E., Molle, D., Larochette, N., Zamzami, N., Jan, G., Kroemer, G., Brenner, C., 2007. GAPDH, a novel regulator of the pro-apoptotic mitochondrial membrane permeabilization. Oncogene 26, 2606–2620.
Tomassini, B., Malisan, F., Franchi, L., Nicolo, C., Calvo, G.B., Saito, T., Testi, R., 2004. Calnexin suppresses GD3 synthase-induced apoptosis. FASEB J. 18, 1553–1555.
Tsang, K.Y., Chan, D., Bateman, J.F., Cheah, K.S., 2010. In vivo cellular adaptation to ER stress: survival strategies with double-edged consequences. J. Cell Sci. 123, 2145–2154.
Voltan, R., Secchiero, P., Corallini, F., Zauli, G., 2014. Selective induction of TP53I3/p53-inducible gene 3 (PIG3) in myeloid leukemic cells, but not in normal cells, by Nutlin-3. Mol. Carcinog. 53, 498–504.
Wagner, W., Ho, A.D., Zenke, M., 2010. Different facets of aging in human mesenchymal stem cells. Tissue Eng. Part B Rev. 16, 445–453.
Wagner, W., Horn, P., Castoldi, M., Diehlmann, A., Bork, S., Saffrich, R., Benes, V., Blake, J., Pfister, S., Eckstein, V., et al., 2008. Replicative senescence of mesenchymal stem cells: a continuous and organized process. PLoS One 3, e2213.
Wang, J., Liao, L., Tan, J., 2011. Mesenchymal-stem-cell-based experimental and clinical trials: current status and open questions. Expert. Opin. Biol. Ther. 11, 893–909.
Will, M.B., 2010. Gene expression profiling of mesenchymal stem cells aged in vitro. Doctoral Dissertation. University of Glasgow (http://theses.gla.ac.uk/id/eprint/1964).

Yi, T., Song, S.U., 2012. Immunomodulatory properties of mesenchymal stem cells and their therapeutic applications. Arch. Pharm. Res. 35, 213–221.
Yi, W., Sun, Y., Wei, X., Gu, C., Dong, X., Kang, X., Guo, S., Dou, K., 2010. Proteomic profiling of human bone marrow mesenchymal stem cells under shear stress. Mol. Cell. Biochem. 341, 9–16.
Zhang, J., Nuebel, E., Daley, G.Q., Koehler, C.M., Teitell, M.A., 2012. Metabolic regulation in pluripotent stem cells during reprogramming and self-renewal. Cell Stem Cell 11, 589–595.
Zou, L., Ding, Z., Roy, P., 2010. Profilin-1 overexpression inhibits proliferation of MDA-MB-231 breast cancer cells partly through p27kip1 upregulation. J. Cell. Physiol. 223, 623–629.